Journal of Molecular and Cellular Cardiology 100 (2016) 54–63

Contents lists available at ScienceDirect

Journal of Molecular and Cellular Cardiology

journal homepage: www.elsevier.com/locate/yjmcc

S100A4 protects the myocardium against ischemic stress☆

Shirin Doroudgar, PhD [a,b,c], Pearl Quijada, PhD [a], Mathias Konstandin, MD [a,b,c], Kelli Ilves, BS [a], Kathleen Broughton, PhD [a], Farid G. Khalafalla, PhD [a], Alexandria Casillas [a], Kristine Nguyen [a], Natalie Gude, PhD [a], Haruhiro Toko, MD [a], Luis Ornelas, BS [a], Donna J. Thuerauf, MS [a], Christopher C. Glembotski, PhD [a], Mark A. Sussman, PhD [a], Mirko Völkers, MD [a,b,c,*]

[a] The San Diego State Heart Institute and Department of Biology, San Diego State University, San Diego, CA 92182, USA
[b] University Hospital Heidelberg, Internal Medicine III, Heidelberg, Germany
[c] DZHK (German Centre for Cardiovascular Research), partner site Heidelberg/Mannheim, Germany

ARTICLE INFO

Article history:
Received 23 March 2016
Received in revised form 13 September 2016
Accepted 4 October 2016
Available online 6 October 2016

Keywords:
S100A4
Myocardial infarction
Remodeling

ABSTRACT

Background: Myocardial infarction is followed by cardiac dysfunction, cellular death, and ventricular remodeling, including tissue fibrosis. S100A4 protein plays multiple roles in cellular survival, and tissue fibrosis, but the relative role of the S100A4 in the myocardium after myocardial infarction is unknown. This study aims to investigate the role of S100A4 in myocardial remodeling and cardiac function following infarct damage.
Methods and results: S100A4 expression is low in the adult myocardium, but significantly increased following myocardial infarction. Deletion of S100A4 increased cardiac damage after myocardial infarction, whereas cardiac myocyte-specific overexpression of S100A4 protected the infarcted myocardium. Decreased cardiac function in S100A4 Knockout mice was accompanied with increased cardiac remodeling, fibrosis, and diminished capillary density in the remote myocardium. Loss of S100A4 caused increased apoptotic cell death both in vitro and in vivo in part mediated by decreased VEGF expression. Conversely, S100A4 overexpression protected cells against apoptosis in vitro and in vivo. Increased pro-survival AKT-signaling explained reduced apoptosis in S100A4 overexpressing cells.
Conclusion: S100A4 expression protects cardiac myocytes against myocardial ischemia and is required for stabilization of cardiac function after MI.

1. Introduction

The progressive nature of ischemic cardiomyopathy appears to be dictated partly by the continuous loss of cardiac myocytes and the inability of the myocardium to regenerate [1]. New treatments that target the disease mechanism at the cellular and whole-organ level are needed to halt and reverse the devastating consequences of this disease. S100A4 is a calcium-binding cardiac protein shown to protect cardiac myocytes from cell death [1,2]. S100 proteins constitute of EF-hand calcium-binding proteins that regulates biological processes, such as cardiac contractility, proliferation, migration, and cell differentiation [3]. S100A4 was first described as a factor promoting metastasis and angiogenesis [4,5]. The mechanisms of these effects are not fully elucidated, but it is well known that the protein has both intracellular and extracellular functions, and that the molecular pathways and mechanism are mediated, at least partly, by activation of the pro-survival kinase AKT [6,7]. Importantly, in the last years S100A4 was related to multiple functions including cardiomyogenesis, growth and also survival promoting activity on cardiac myocytes [1,2,8]. Moreover, S100A4-Cre-recombinase reporter mice have been used for fibroblast lineage tracing in the myocardium, although specificity of S100A4 for cardiac fibroblasts has been recently questioned [2,9,10]. More recently it has been shown that S100A4 knockout mice showed reduced interstitial fibrosis, decreased myofibroblasts, suppressed expressions of collagens and pro-fibrotic cytokines in the left ventricle after pressure overload [3,11]. However, no studies have examined the effects of increased S100A4 protein levels in the ischemic myocardium. Therefore, acute myocardial infarction (MI) was used as the setting to assess the impact of S100A4 on pathologic injury using knockout and overexpression models, with implications for S100A4 as a novel therapeutic target for cardiac ischemia.

2. Methods

2.1. Animal procedures, echocardiography and invasive hemodynamics assessment

Generation of S100A4 null mice was previously reported [4,5,12]. Eight-ten week-old male S100A4 KO and wild-type (WT) mice of an A/Sn genetic background were used for the present study. The mice

☆ Subject codes: Basic Science Research (130), Other Myocardial Biology (108).

* Corresponding author at: University Hospital Heidelberg, Department of Internal Medicine III, Im Neuenheimer Feld 669, 69120 Heidelberg, Germany.
E-mail address: Mirko.voelkers@med.uni-heidelberg.de (M. Völkers).

http://dx.doi.org/10.1016/j.yjmcc.2016.10.001
0022-2828/

were housed 8–10 animals/cage with a 12-hour light and dark cycle and were fed standard laboratory chow and water ad libitum. Myocardial infarction was produced by ligating the left anterior descending (LAD) branch of the coronary artery using a 8-0 suture (Ethicon). Control mice underwent a sham operation. Echocardiography was performed under mild isoflurane sedation (0.5%–1.5%) using a Vevo 770 high-resolution system. Cardiac function was analyzed in the parasternal long axis view by tracking the endocardium with the supplied analysis software to obtain end systolic volume, end diastolic volume, ejection fraction, and heart rate. Consecutive noninvasive assessment of cardiac function in the parasternal long axis view has been performed 1, 2, 4, and 6 weeks after surgery. Closed chest hemodynamic assessment was performed on mice anesthetized with 3% chloral hydrate (10 μL per 1 mg body weight) before insertion of microtip pressure transducer (FT111B, Scisense) into the right carotid artery and advancement into left ventricle. The catheter was connected to an A/D converter (FV892A, Scisense) for data collection. After hemodynamic measurements, hearts were arrested in diastole using high potassium solution

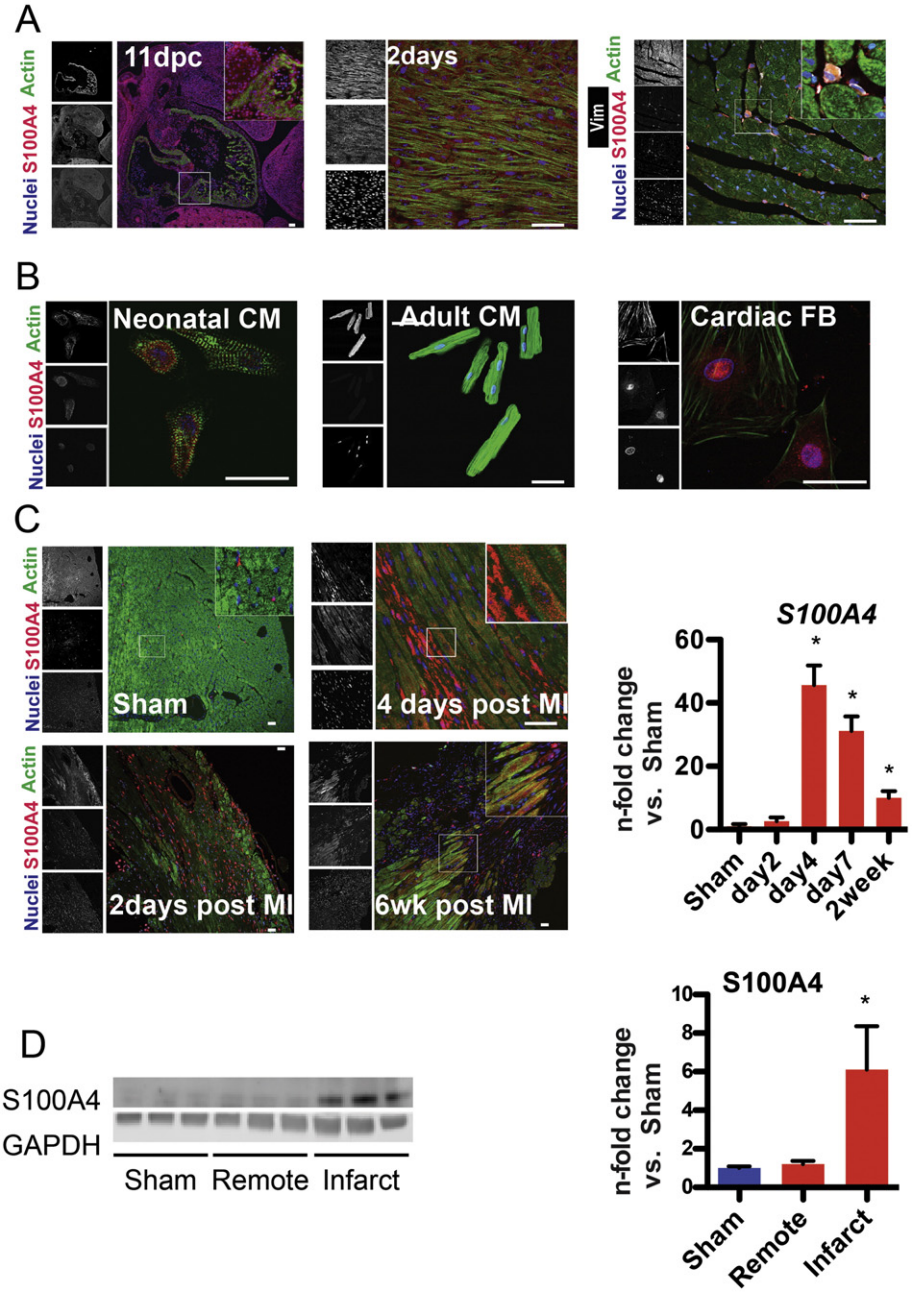

Fig. 1. S100A4 in development and after myocardial infarction. (A) Confocal microscopy of paraffin-embedded sections from wild-type mouse hearts at 11 dpc, 2 days and 3 months stained for S100A4 (red), Actin (green), Vimentin (white) and nuclei (blue) at different developmental stage. S100A4 is highly expressed in embryonic hearts, but only expressed in interstitial cells in adult myocardium. Scale bar 25 μM. (B) Immunofluorescence in neonatal cardiomyocytes (CM) (left panel) show robust expression of S100A4 whereas adult myocytes (middle panel) are negative for S100A4. Strong S100A4 expression is observed in cardiac Fibroblast (FB - right panel). Scale bar 25 μM. (C) Confocal microscopy of paraffin-embedded sections from wild-type mouse hearts at sham operated, 2 days, 4 days and 6 weeks post MI stained for S100A4 (red), Actin (green), Scale bar 25 μM. Right: S100A4 transcription in hearts of mice of the indicated group after surgery. *$p < 0.01$ versus Sham. $n = 4$ per group. Scale bar 25 μM. (D) Immunoblot and quantification for S100A4 in infarcted myocardium (6 weeks after Infarction). *$p < 0.01$ versus Sham. $n = 3$ per group.

Table 1
Echocardiographic and morphometric characterization of 10 week old mice.

		WT	S100A4 KO
		n = 4	n = 4
10 week old	LVEDV, μl	49.24 ± 5.817	52.98 ± 9.822
	EF,%	53.88 ± 4.859	54.13 ± 27.160
	HR, bpm	492 + ±23	497 ± 19
	HW/BW mg/g	4.54 + ±0.25	4.58 ± 0.27

Characterization of mice after Sham or MI by morphometry and echocardiography. Abbreviations: n: number of mice analyzed; LVEDV, μl: left ventricular end diastolic volume; EF, %: ejection fraction. HR, bpm: Heart rate; dP/dt: first derivative of left ventricular pressure. BW, body weight; HW: heart weight; HW/BW: heart weight/body weight ratio.

and perfused with phosphate-buffered formalin for 15 min (Sigma-Aldrich) via retrograde cannulation of the abdominal aorta. Retroperfused hearts were removed from the chest cavity and placed in formalin for at least another 24 h. Alternatively, after hemodynamic assessment hearts were removed directly and frozen down in liquid nitrogen until further processing.

2.2. Tissue collection

We sacrificed mice at various time points after MI or sham operation and removed the hearts. For later isolation of RNA and protein in the MI study, left ventricles were divided into the infarcted area (apex, distal to the ligation site) and the non-infarcted remote myocardium (basal part of the interventricular septum) and stored in in liquid N2.

2.3. Immunohistochemistry

Please find a detailed protocol in the online-only Data supplement.

2.4. Infarct size measurements

Paraffin sections were stained with tropomyosin to visualize live myocardium and TO-PRO-3 iodide to determine nuclei distribution and area of infarction. Area of live myocardium was measured using an outlining tool supplied by the Leica Imaging software and normalized to the total area of the left ventricular free wall and converted to a percentage.

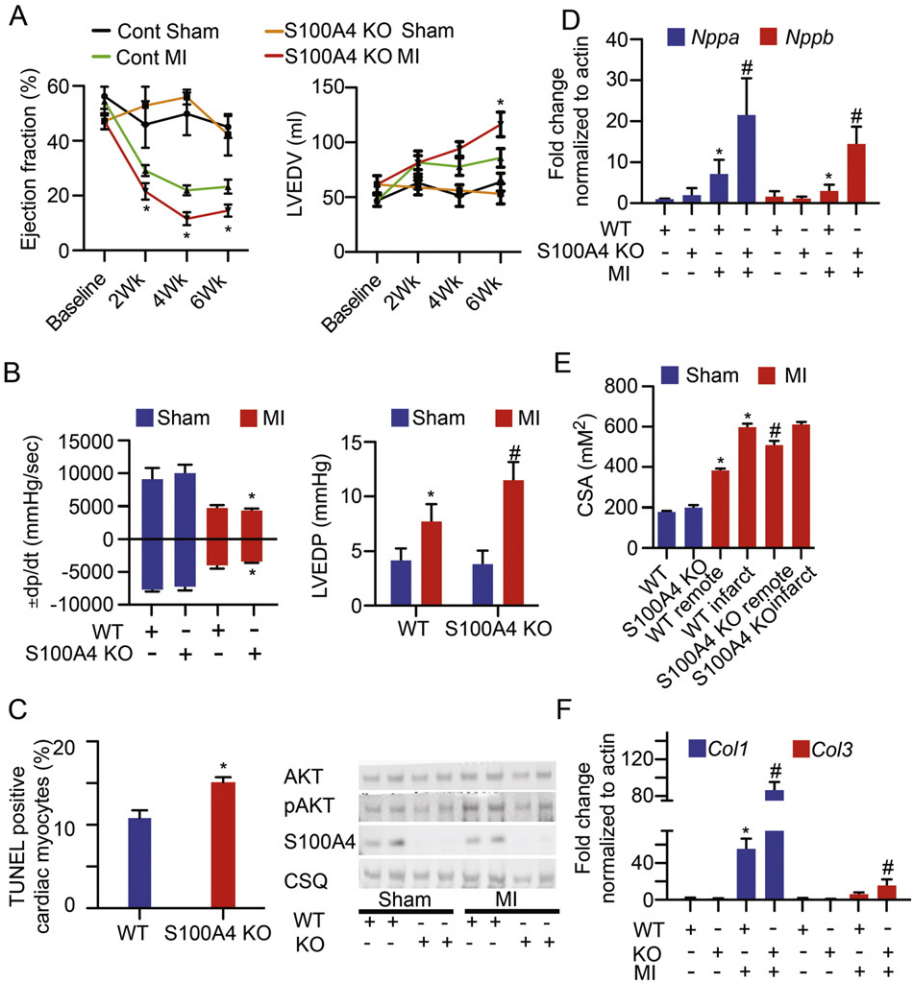

Fig. 2. Impact of S100A4 deletion on cardiac function after infarction. (A) Mice were infarcted at 8–10 weeks of age where cardiac function was unchanged between WT and S100A4 KO mice. Echocardiographic assessment of WT and S100A4 KO hearts for EF and left ventricular end-diastolic volume (LVEDV). *p < 0.05 versus WT MI. n = 6 per group. (B) In vivo hemodynamic measurements of ±dP/dT and left ventricular enddiastolic pressure 6-weeks post-surgery. *p < 0.05 versus WT MI. n = 6 per group. (C) Percentage of TUNEL-labeled myocytes in the left ventricle in the border zone area 1 d after MI. n = 4 per group, *p ≤ 0.05 vs Control MI. Error bars indicate means ± sem. n = 4 per group. Right Panel: Immunoblots for indicated proteins in control and S100A4 KO mice. (D) ANP and BNP transcription in hearts of mice of the indicated group 6 weeks after surgery. *p < 0.01 versus WT, # < 0.05 vs WT Co MI. n = 6 per group. (E) Myocyte cross sectional area (CSA) in control and S100A4 KO mice 6 weeks after surgery. *p < 0.01 versus WT sham; #p < 0.05 versus WT remote. Error bars indicate means ± sem. n = 4 per group. (F) Collagen 1 and Collagen3 transcription in hearts of mice of the indicated group 6 weeks after surgery. *p < 0.01 versus Control. Error bars indicate means ± sem. n = 6 per group.

2.5. Myocyte size measurements

Paraffin sections were stained for tropomyosin to visualize live myocardium wheat germ agglutinin-488 (Carlsbad, Invitrogen) to outline cardiomyocyte membrane and TO-PRO-3 to visualize nuclei. Myocytes were measured using a ImageJ to measure area as μm^3. An n = 4 per group was measured.

2.6. Cardiomyocyte cell culture and treatment

Neonatal Ventricular cardiomyocytes from 1- to 2 d-old rat neonatal hearts (NRCMs) were prepared by trypsin digestion using standard procedures. Cell suspensions were pre-plated for 2 h in M199 medium (Cell-Gro) supplemented with 15% fetal bovine serum (FBS) to reduce non-myocyte cell contamination. Myocytes were plated in gelatin (Sigma) precoated 10 cm dishes or in laminin (Sigma) precoated glass slides using the preplating media.

2.7. Conditioned media studies and apoptosis assays

Fibroblast cultures from Wildtype and S100A4 KO mice were washed thoroughly with phosphate-buffered saline and allowed to condition fresh serum-free (control) media for 24 h. The resultant fibroblast conditioned media were filtered through a 0.22 μm filter to remove any cellular debris and added to NRCMs previously cultured in control media. After 3 h, conditioned cell death was induced by challenge with H_2O_2 (50 μM for 3 h).

For isolation of adult myocytes, following chloral hydrate anesthesia (400 mg/kg body weight, i.p.), the heart was excised and left ventricular (LV) myocytes were enzymatically dissociated 11. The myocardium was perfused retrogradely through the aorta at 37 °C with a Ca^{2+} free solution. At completion of digestion, the LV was cut in small pieces and resuspended in Ca^{2+} 0.1 mM solution. Cells were maintained in M199 for 24 h at 37 °C, 95%O_2, 5%CO_2 and used for further analysis after medium exchange.

2.8. Invasion assay

Fibroblast invasion was quantified using a modified two-chamber invasion assay (membrane coated with a layer of Matrigel extracellular matrix proteins) according to the manufacturer's instructions (BD Bioscience). The bottom chamber was filled with 750 μL M199 medium (Cell-Gro) supplemented with 15% fetal bovine serum (FBS), and the insert was placed into the media. Cells suspended in serum free culture media was seeded in the top insert. The cells were allowed to invade for 24 h at 37 °C. Cells attaching to the lower surface of the membrane were fixed and stained. Quantification was performed by counting the stained cells under light microscopy.

2.9. siRNA transfection

NRCM were transfected with small interfering RNAs (siRNAs, 100 nM) by using HiPerfect transfection reagent (Qiagen) as per the manufacturer's recommendations. After incubation for 5–10 min, transfection complexes were added to the cells for 48 h. The following siRNA sequences were used: rat S100A4 siRNA:

Sense: 5′ U.G.A.A.C.A.A.C.U.U.G.G.A.C.A.G.C.A.A.U.U 3′.

Antisense: 5′ U.U.G.C.U.G.U.C.C.A.A.G.U.U.G.U.U.C.A.U.U 3′. The control siRNA was obtained from Ambion.

2.9.1. Adeno-associated virus serotype 9 generation and systemic in vivo AAV9 cardiac- targeted gene transfer protocol

In vivo cardiac-targeted S100A4 expression in normal mouse hearts was obtained by using tail vein injection of an adeno-associated virus serotype 9 (AAV9) harboring the S100A4 gene driven by a cardiomyocyte-specific CMV-MLC2v0.8 promoter. Recombinant AAV9 vector carrying the same promoters without a downstream encoded transgene product served as control. Adult male C57BL/6 mice were anesthetized with isoflurane (2%) and 100 μL of 37 °C heated Ringer Lactate containing 1×10^{11} total viral particles of either AAV9-control, AAV9-S100A4 as previously described [6,7,13].

2.10. Real-time RT-PCR

Total RNA was isolated from frozen heart or cultured cells by using Quick-RNA™ MiniPrep (Zymo Research) and reverse-transcribed into complementary DNA (cDNA) by using High Capacity cDNA Reverse Transcription Kit (Applied Biosystems). Real-time PCR was performed on all samples in triplicate using QuantiTect™ SYBR Green PCR Kit (Qiagen) according to the manufacturer's instructions. All primer sequences are shown in Supplemental Table 1 of the Online Data Supplement.

2.11. Immunoblotting

Immunoblotting was performed using standard procedures. Protein lysates from ventricles or cultured cardiomyocytes were loaded onto a 4–12% NuPAGE Novex Bis-Tris Gel (Invitrogen) for electrophoresis.

Table 2
Echocardiographic and morphometric characterization 2 weeks and 6 weeks after surgery.

		Sham		MI	
		WT	S100A4 KO	WT	S100A4 KO
		n = 4	n = 4	n = 13	n = 12
2 week after	LVEDV, μl	71.44 ± 26.75	64.77 ± 2.73	109.5 ± 7.96	97.18 ± 24.59
	EF, %	41.67 ± 2.180	41.39 ± 2.69	29.07 ± 2.92*	21.70 ± 1.519#
	HR, bpm	424 ± 12	448 ± 14	471 ± 14	440 ± 23
		WT	S100A4 KO	WT	S100A4 KO
		n = 10	n = 10	n = 13	n = 12
6 weeks after	LVEDV, μl	73.99 ± 4.967	66.56 ± 8.83	90.46 ± 7.94	116.3 ± 11.26#
	EF,%	45.05 ± 3.990	42.22 ± 7.54	23.28 ± 2.56*	14.56 ± 2.16#
	+dP/dt	9108 ± 1693	10,026 ± 1298	5661 ± 359.4*	4513 ± 291#
	−dP/dt	7678 ± 291	7249 ± 581	4951 ± 292*	3607 ± 238#
	HW/BW mg/g	4.71 + ±0.3	4.2 ± 0.34	5.3 + ±0.2*	5.2 ± 0.19*

Characterization of mice after Sham or MI by morphometry and echocardiography. Abbreviations: n: number of mice analyzed; LVEDV, μl: left ventricular end diastolic volume; EF, %: ejection fraction. HR, bpm: Heart rate; dP/dt: first derivative of left ventricular pressure. BW, body weight; HW: heart weight; HW/BW: heart weight/body weight ratio.

* $p < 0.05$ vs Sham.

\# $p < 0.05$ vs WT MI.

Separated proteins were then transferred onto a polyvinylidene fluoride (PVDF) membrane, blocked with 5% skim milk in Tris-Buffered Saline Tween-20 (TBST) for 1 h at room temperature, and exposed to primary antibodies. Alkaline phosphatase (AP), horseradish peroxidase (HRP) or Cy5-conjugated IgG (Jackson ImmunoResearch, West Grove, PA) were used as secondary antibodies. Fluorescence signal was detected and quantified by using a Typhoon 9400 fluorescence scanner together with ImageQuant 5.0 software (Amersham Biosciences).

2.12. Flow cytometry

NRCM were stained with Annexin V (BD Biosciences) and Sytox blue (Invitrogen) according to the manufacturer's instructions. Cell pellet was collected by trypsinization and centrifugation, then incubated with Annexin V (1:50) and Sytox blue (1:1000) for 15 min. Annexin V has a high affinity for the membrane phospholipid phosphatidylserine which is exposed to the external environment during early apoptosis. Sytox Blue is a high-affinity nucleic acid stain that easily penetrates cells with compromised plasma membranes but will not cross intact membranes in viable cells. Flow cytometry was performed by using a BD FACSAria Flow Cytometer (BD Biosciences).

2.13. Cell proliferation

Cell proliferation was determined using the CyQuant proliferation assay from Invitrogen according the manufacturer's instruction. Briefly, 1000 Fibroblasts in 100 μL per well were seeded in a 96-well flat bottom plate. Assay was initiated by addition of 100 μL of CyQUANT direct (Invitrogen) green fluorescent nucleic acid stain in each well and incubated for 30 min. Green fluorescence intensity was measured at 495 nm using a plate reader and represented as fold change to the fluorescence intensity measured on the day of plating (day 0, ≥8 h after plating). Subsequent measurements were determined at the indicated days.

2.14. Statistical analysis

Statistical analysis was performed with GraphPad Prism 5.0 (GraphPad Software Inc.; www.graphpad.com). Values of $p < 0.05$ were considered significant. All the data sets were tested for normality of distribution with the Shapiro-Wilk test. To compare 2 groups with normal distribution, the Student *t*-test was applied; otherwise, a non-parametric test was used. Nonparametric tests were used when $n < 5$ per group. For comparison of >2 groups, 1-way ANOVA was applied;

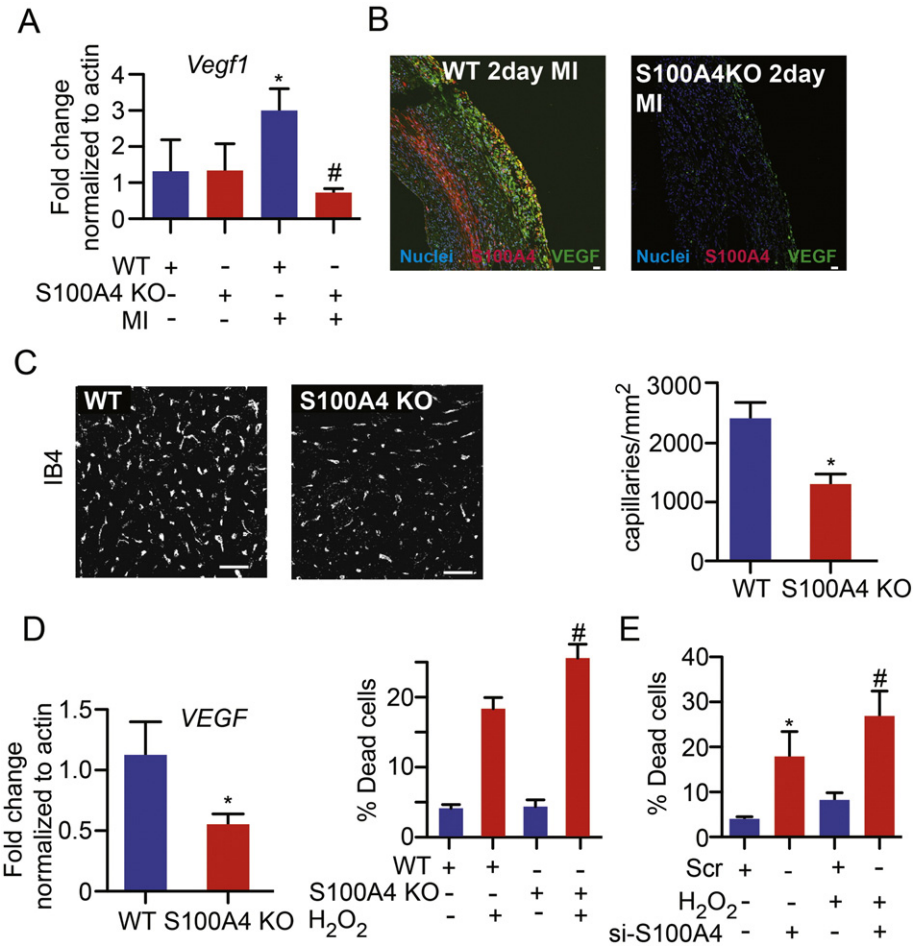

Fig. 3. Impact of S100A4 deletion on angiogenic response and cell death. (A) VEGF transcription in mice 6 week after surgery. *$p < 0.01$ versus control sham; #$p < 0.05$ versus control MI). Error bars indicate means ± sem. n = 3 per group. (B) Confocal microscopy of paraffin-embedded sections from wild-type and S100A4 KO mice hearts at 2 days post MI stained for S100A4 (red), VEGF (green) and nuclei (blue). S100A4 is only expressed in control hearts. Decreased VEGF expression in S100A4 KO mice. Scale bar 25 μM. (C) Immunohistochemistry showing endothelial cells 6 weeks after vessel ligation detected by cell type-specific staining (IsolectinB4-IB4) (left panel). Scale bar 25 μM. Quantification of capillaries or the analyzed area (n = 6–7); for each heart 6 fields were counted. *$p < 0.01$ versus control. Error bars indicate means ± sem. (D) Left panel: VEGF transcription in isolated fibroblasts. *$p < 0.05$ versus WT. Right panel: Cardiac myocytes were incubated with conditioned Media from WT or S100A4 KO fibroblast for 3 h and challenged with H_2O_2. Cell death was quantified by flow cytometric detection of annexin and 7-amino-actinomycin D (7-AAD) staining. $p < 0.05$ versus WT; #$p < 0.05$ versus WT H_2O_2. Error bars indicate means ± sem. n = 4 independent experiments. (E) Small interfering RNA (siRNA) knockdown of S100A4 in NRCMs increases cell death in response to H_2O_2. $p < 0.05$ versus Scr; #$p < 0.05$ versus Scr H_2O_2. n = 3 independent experiments.

for the echocardiographic time course analysis, repeated measures ANOVA was used. Bonferroni post hoc tests were included in both cases.

3. Results

3.1. S100A4 expression in the myocardium

Previously, it has been reported that S100A4 protein expression is upregulated in cardiac myocytes under ischemic conditions, and this increased expression of S100A4 has been linked to improved survival and growth of myocytes [2]. S100A4 expression was first confirmed by confocal immunocytofluorescent microscopy. S100A4 is highly expressed in embryonic and postnatal cardiac myocytes, but absent in adult cardiac myocytes (Fig. 1A) and only few S100A4-positive cells were present in the myocardium. Similarly, S100A4 expression is high in isolated neonatal rat cardiac myocytes (NRCM) and neonatal rat cardiac fibroblast (FB), whereas adult rat cardiac myocytes (ARCM) are negative for S100A4 immunostaining (Fig. 1B). Numbers of S100A4 positive cells increased following permanent occlusion of the left anterior descending (LAD) coronary artery at two days post-myocardial infarction (MI) (Fig. 1C). S100A4 expression was measured by RT-PCR and immunohistochemistry at different time points. S100A4 peaked at day 4 after myocardial infarctions (Fig. 1C). Immunohistochemistry confirmed expression of S100A4 in cardiomyocytes 4 days after myocardial infarction and cardiac myocytes showed strong S100A4 staining in the infarct border zone at six weeks post myocardial infarction. S100A4 expression in the myocardium was confirmed by immunoblots (Fig. 1D). Similar to the immunohistochemistry, S100A4 expression increased (6-fold) in the infarcted myocardium. The increased expression of S100A4 prompted to test the hypothesis that increased S100A4 protein expression protects cardiac myocytes, and that cardiac-specific overexpression of S100A4 is beneficial to the myocardium after myocardial infarction.

3.2. S100A4 depletion results in cardiac dysfunction

To further understand the relevance of S100A4, in vivo, S100A4 Knockout (S100A4 KO) mice were obtained and characterized [12]. S100A4 KO mice do not show any obvious phenotype at birth and develop normally. S100A4 KO mice have no cardiac abnormalities for the first 3 months after birth, as cardiac function and morphology was unchanged in 10 week-old male S100A4 KO mice compared to wildtype (WT) mice assessed by echocardiography (Table 1), but develop dilated cardiomyopathy at one year of age (Supplemental Fig. 1). Since S100A4 is not present in adult healthy cardiomyocytes, we explored phenotypic alterations after S100A4 loss in isolated cardiac fibroblasts.

First, the invasive phenotype of fibroblasts was assessed using a Matrigel based invasion assay. Fibroblasts isolated from S100A4 KO mice were compared to WT fibroblasts. S100A4 KO fibroblast showed a decreased invasive capacity compared to WT control fibroblasts, which was associated with decreased expression of Matrix metalloproteinases (MMPs), and extracellular matrix proteins like Tenascin C. In line with previous reports, S100A4 deletion caused decreased expression of vascular endothelial growth factor (VEGF) both in vitro and in vivo (Supplemental Fig. 1). Adenoviral expression of S100A4 in S100A4 KO cells rescued this phenotype (Supplemental Fig. 2). Overall proliferation of fibroblast was unaffected by S100A4 KO but increased after S100A4 overexpression (Supplemental Fig. 2), which was associated with an increased expression of Matrix metalloproteinases (MMPs) and VEGF.

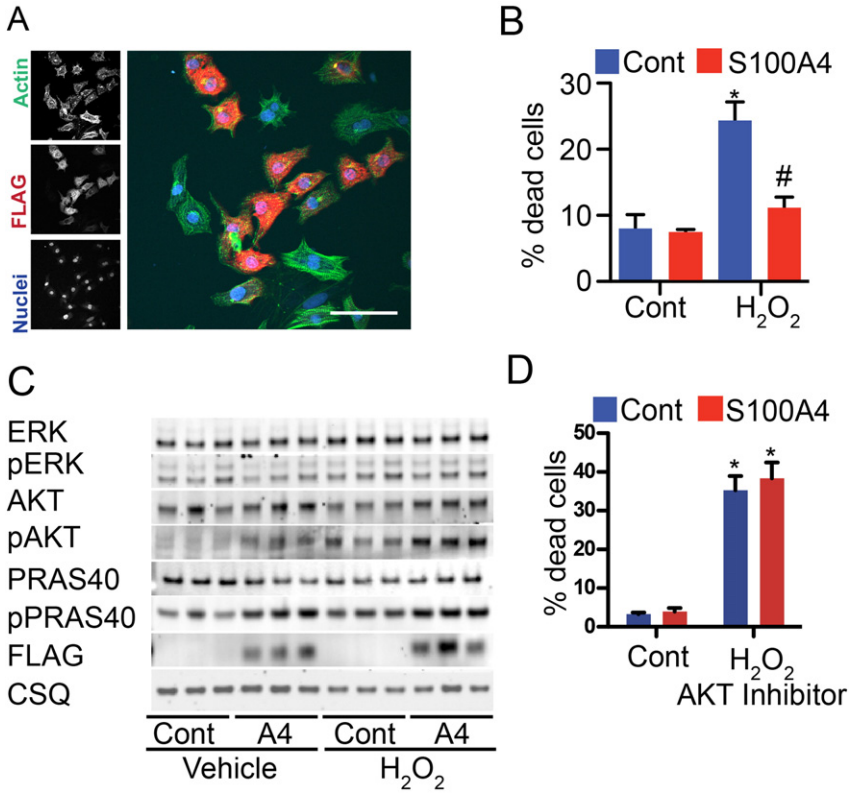

Fig. 4. Impact of S100A4 Overexpression on cell death. (A) Immunofluorescence of myocytes stained for FLAG/S100A4 (red), Actin (green) and nuclei (blue). Scale bar 25 μM. (B) Overexpression of S100A4 in NRCMs decreases cell death in response to H_2O_2. $p < 0.05$ versus Control; #$p < 0.05$ versus Control H_2O_2. $n = 3$ independent experiments. Error bars indicate means ± sem. (C) Immunoblots for indicated proteins in control and S100A4 treated myocytes. (D) Cell death quantified by flow cytometric detection on H_2O_2. treatment. AKT Inhibition (Akt inhibitor V 5 μM) blunts the protective effects of S100A4. *$p < 0.05$ vs control H_2O_2.

Next, at the age of 10 weeks, both S100A4 KO and control mice underwent sham or MI surgery. Cardiac function in control and KO mice declined after MI. However, by 2 weeks after MI, heart function in KO mice exacerbated compared with control mice, as evidenced by ejection fraction values measuring 21% versus 29% at 2 weeks after MI (Fig. 2A). End diastolic volume was higher in KO mice at 6 weeks post MI, indicating pronounced cardiac dilatation. Heart rates were not different between groups after MI (Table 2). Invasive hemodynamic assessment at the end of the follow-up period confirmed these data, as positive and negative developed pressures were significantly impaired in the KO animals (Fig. 2B). Also, end diastolic pressure, was higher in KO animals compared with controls 6 weeks after MI (Fig. 2B). Increased cell death after myocardial infarction might be contributing to the decreased cardiac function in S100A4KO mice. While 10% of the cardiac myocytes in the border zone were TUNEL positive in control mice, S100A4KO increased apoptotic cells to 15% (Fig. 2C). Missing S100A4 expression in S100A4KO mice was confirmed by immunoblots (Fig. 2C). In line with previous published data, S100A4 KO decreased AKT phosphorylation, in vivo (Fig. 2C). Cardiac remodeling was exacerbated in S100A4 knockout animals compared to control animals as assessed by increased hypertrophic gene signature (Fig. 2D). In addition, cardiomyocyte cross-sectional area was increased in KO animals (Fig. 2E). Fibrotic remodeling was exacerbated in S100A4 knockout animals compared to control animals as assessed by increased collagen expression (Fig. 2F). Collectively, these data show that deletion of S100A4 increases ischemic injury and adverse remodeling following myocardial infarction.

3.3. Loss of S100A4 attenuates capillary density

Molecular mechanisms for S100A4-mediated increase in ischemic injury were analyzed in the early phase after MI. S100A4 is known for its role in angiogenesis, and VEGF was recently found as the most upregulated gene among chemokines by S100A4-positive cells during metastasis [5]. VEGF1 expression increased 3-fold 2 days after MI in control mice. In contrast, increase in VEGF expression was blunted in S100A4 KO mice (Fig. 3A). Increased VEGF expression in control mice compared to knockout animals was confirmed by immunofluorescence (Fig. 3B). The VEGF positive cell population after myocardial infarction was located close to the epicardium, whereas many S100A4 positive, but VEGF negative cells, localized in the midventricular area. However, many VEGF positive cells in the epicardial area are also S100A4 positive. Consistently, capillary density was significantly lower in knockout animals following myocardial infarction, as assessed by staining for isolectinB4 (IB4-endothelial cells) (Fig. 3C). Next, cardiac fibroblasts form S100A4 knockout animals were isolated. VEGF expression was reduced in knock out fibroblast compared to control cells, in line with the in vivo data (Fig. 3D). Adult cardiomyocytes are negative for S100A4

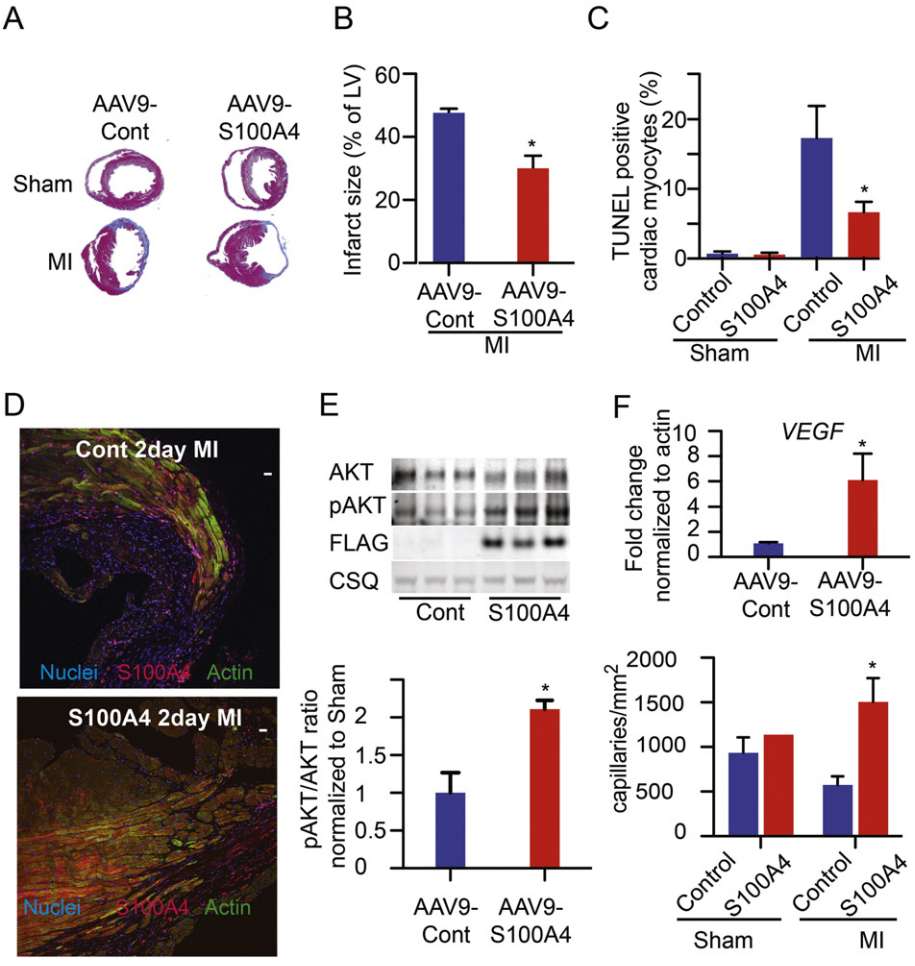

Fig. 5. Impact of S100A4 overexpression on cardiac remodeling after infarction. (A) Masson-Trichrome Staining Control and S100A4 treated hearts 6 weeks after surgery. (B) Infarct size measurements 6 weeks after MI. *$p < 0.05$ versus Control MI. Error bars indicate means ± sem. n = 4 per group. (C) Percentage of TUNEL-labeled myocytes in the left ventricle in the border zone area 1 d after MI. n = 5 per group, *$p < 0.05$ vs Control MI. Error bars indicate means ± sem. (D) Immunohistochemistry confirmed overexpression of S100A4. Confocal microscopy of sections from control hearts and S100A4 treated hearts 6 weeks after MI stained for S100A4 (red), Actin (green) and nuclei (blue). Scale bar 25 μM. (E) Immunoblots and quantification in control and S100A4 treated myocytes. (F) VEGF transcription in mice 6 week after surgery. *$p \leq 0.01$ versus control. Error bars indicate means ± sem. n = 3 per group. Quantification of capillaries or the analyzed area. For each infarcted heart 4–6 fields were counted. *$p \leq 0.05$ versus control. Error bars indicate means ± sem.

expression. Therefore, the effect of S100A4 depletion in cardiac fibroblasts on myocyte viability was first tested with conditioned media from knockout and control cardiac fibroblasts. Neonatal rat cardiac myocyte (NRCM) cultures were incubated in the conditioned medium for 3 h in serum-depleted conditions. Cultures of NRCMs in conditioned medium from S100A4 knockout cells showed a significant increase in the percentage of dead cells after challenge with H_2O_2, based on flow cytometric analysis of apoptotic and necrotic markers (Fig. 3D). To test whether S100A4 has direct functional impact on cardiac myocyte viability, NRCMs were depleted from S100A4 using siRNAs. NRCMs were stressed by H_2O_2 treatment, and resultant cell death was quantified using nuclear staining with 7-amino-actinomycin D and annexin, followed by fluorescence-activated cell sorter analysis. H_2O_2 stress resulted in increased cell death in S100A4 knockdown cells, compared with control siRNA-treated cultures (Fig. 3E). This data further suggest that S100A4 mediates pro-survival signaling in response to ischemia.

3.4. S100A4 prevents cell death

To understand the mechanism of S100A4-mediated protection in cardiac myocytes, in vitro experiments were performed. It has been previously reported that S100A4 can influence AKT signaling [14,15]. Furthermore, recent studies showed a neuro-protective role of S100A4, which was in part dependent on increased AKT signaling [16,17]. To mimic enhanced S100A4 expression the role of intracellular S100A4 in apoptotic signaling were examined using adenoviral vector carrying FLAG-tagged cDNA encoding wild-type S100A4, or a control empty vector (Fig. 4A). Cultures of NRCM overexpressing S100A4 showed a significant reduction in the percentage of dead cells after challenge with H_2O_2 (Fig. 4B). In line with the previous results, H_2O_2 challenge increased AKT phosphorylation and AKT targets such as PRAS40 in control myocytes (Fig. 4C). This phosphorylation was further increased in S100A4-overexpressing NRCMs. Consistent with these results, myocytes incubated with an AKT inhibitor (AKT Inhibitor V) lose the protective effect of S100A4 against oxidative stress (Fig. 4D). In contrast, phosphorylation of the MAP kinase, ERK, was unchanged in S100A4 myocytes (Fig. 4C).

3.5. S100A4 protects against infarction injury

A cardio-protective role for S100A4 was examined, in vivo, using mice injected with either control or S100A4 adeno-associated virus serotype 9 (AAV9). Expression of other S100 proteins were not affected after S100A4 overexpression (Supplemental Fig. 2). Control and S100A4 expressing mice were subjected to permanent ligation of the left coronary artery. Infarct size was reduced in S100A4 mice compared to control mice (Fig. 5A–B). Decreased cell death in the border zone might be contributing to the decreased infarct size in S100A4 mice. Only cells that were both TUNEL positive and α-sarcomeric actin positive were counted. While 16% of the cardiac myocytes in the border zone were TUNEL positive in control mice and S100A4 treatment reduced apoptotic cells to 6% (Fig. 5C). Increased S100A4 expression in AAV9-S100A4 treated mice was confirmed by immunofluorescence (Fig. 5D). In line with the in vitro data, S100A4 increased AKT phosphorylation, in vivo (Fig. 5E). VEGF Expression was increased in the AAV9-S100A4 treated mice, along with an increased capillary density in treated animals following myocardial infarction, as assessed by staining for isolectinB4 (IB4-endothelial cells) (Fig. 5F).

Collectively, this data confirms that selective S100A4 expression in cardiac myocytes protects against ischemic injury, in vivo.

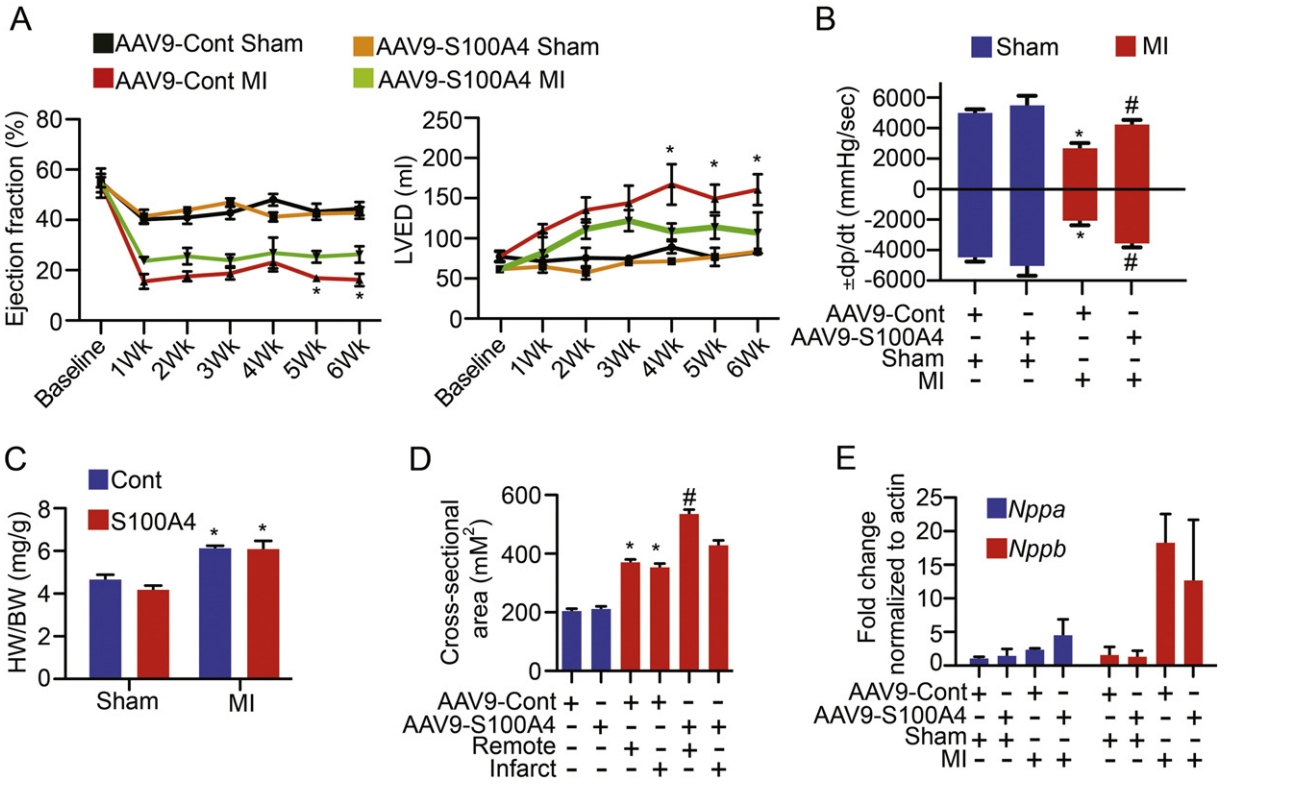

Fig. 6. Impact of S100A4 overexpression on cardiac function after infarction. (A) Echocardiographic assessment of Control or S100A4 hearts for EF, LVEDV. *p < 0.05 versus Control MI. n = 6–7 per group. (B) In vivo hemodynamic measurements of ± dP/dT 6-weeks post-surgery. *p < 0.01 versus Sham. # < 0.05 vs Cont MI. Error bars indicate means ± sem. n = 6–8 mice per group. (C) Heart weight to body weight ratios (HW/BW) in Control and S100A4 mice 6 weeks after sham and MI surgery. *p < 0.01 versus Sham. Error bars indicate means ± sem. n = 4 per group. (D) Myocyte cross sectional area in control and S100A4 mice 6 weeks after surgery (*p < 0.01 versus Control Sham; #p < 0.05 versus Control remote. Error bars indicate means ± sem. n = 4 per group. (E) ANP and BNP transcription in hearts of mice of the indicated group 6 weeks after surgery. *p < 0.01 versus Control. Error bars indicate means ± sem. n = 6 per group.

3.6. S100A4 improves cardiac function after infarction injury

Consequences of ischemic injury on cardiac function were assessed with serial echocardiography. AAV9-S100A4 animals showed significant improvement of ejection fraction. End diastolic dimensions were greater in the control mice compared to S100A4 mice, reflecting accelerated remodeling (Fig. 6A). LV remodeling and dysfunction were exacerbated in the control mice subjected to MI throughout the length of the study (6 weeks). Importantly, heart rate was similar between the groups. Hemodynamic performance was impaired after MI in control animals, but improved in AAV9-S100A4 mice (Fig. 6B). Collectively, this data confirms that selective S100A4 expression in cardiac myocytes protects against ischemic injury and adverse remodeling. Heart weight / body weight ratio increased after MI 1.5-fold both in control mice and S100A4 animals (Fig. 6C). Cross-sectional area was significantly increased in control myocytes subjected to MI, and further significantly increased in AAV9-S100A4 mice, especially in the remote area after myocardial infarction (Fig. 6D), whereas the induction of the hypertrophic gene program was induced similarly in both groups after myocardial infarction (Fig. 6E). Increased hypertrophic response after increased S100A4 expression was also found in isolated cardiomyocytes, where adenoviral overexpression resulted in increased cellular size (Supplemental Fig. 2). This data further suggest that S100A4 improves cardiac function in response to myocardial infarction.

4. Discussion

Prior to this study, no information existed on the functional consequences of increased or decreased S100A4 protein levels in infarcted myocardium. A cardio-protective role for S100A4 in the myocardium following myocardial infarction is supported by findings presented in this study as cardiac myocyte-specific overexpression of S100A4 protects the myocardium after infarction and improves cardiac function. In contrast, global deletion of S100A4 in S100A4 KO mice resulted in decreased cardiac function after myocardial infarction compared to control mice.

4.1. Role of S100A4 signaling in the myocardium

Several studies have demonstrated a correlation between increased numbers of S100A4+ cells and poor prognosis of patients for a variety of cancer types [18]. The metastatic capabilities of $S100A4^{+}$ cancer cells have been studied, however, S100A4 is also expressed by fibroblasts and immune cells, including macrophages in various organs. Little is known about the specific role of S100A4 in the cardiac context. Previous studies showed high S100A4 expression levels in fibroblasts and hematopoietic cells in the myocardium [10,11] and a previous study showed that genetic ablation of S100A4 resulted in suppressed fibrosis after pressure-overload or angiotensin infusion [11], which was associated with altered p53 function in cardiac fibroblasts.

In accordance with previous reports S100A4 expression is high in the developing heart, whereas healthy adult cardiac myocytes were found to express S100A4 at negligible levels (Fig. 1). The mechanism of S100A4 transcriptional regulation in the developing heart are still unknown. Previous work suggested that S100A4 is secreted by parietal endoderm and promotes early differentiation and proliferation of cardiomyocytes [8]. Extracellular S100A4 specially influences transcription in differentiating cardiomyocytes, which could explain the high expression of S100A4 in neonate cardiomyocytes and the absence of expression in fully differentiated adult myocytes.

4.2. S100A4 is in diseased myocardium

Number or S100A4 positive cells increase after myocardial infarction, which explains increased expression after injury. Secretion of S100A4 after inflammatory stimulation has been shown [19] and our data suggest that S100A4 is uptaken in cardiac myocytes in infarct border zone. S100A4 peaks at day 4 after myocardial infarctions and cardiomyocytes become S100A4 positive in the border zone, but are negative at the time of the ischemic results. Although active S100A4 transcription and translation in cardiac myocytes after myocardial infarction cannot be excluded, a previous study showed that myocytes are negative for S100A4 mRNA by in situ hybridization analysis targeting S100A4 mRNA [2]. These findings prompt speculation towards a paracrine protective activity of S100A4 on adult cardiac myocytes. Missing S100A4 or altered secretion of protective factors might explain the increased apoptotic cell death in the S100A4KO mice. Data in this study suggest that altered VEGF signaling may be involved in S100A4-dependent protective effects. Mechanistically, VEGF produced from S100A4-positive cells has been shown to play an important role in the angiogenic environment in metastatic cancers [5]. In line, S100A4 KO mice showed reduced VEGF expression and capillary density after myocardial infarction (Fig. 3), which could contribute to the worsened cardiac function after myocardial infarction as reduced VEGF expression exacerbated cardiac function after myocardial infarction [20,21]. However, many S100A4 positive, but VEGF negative cells, localized also in the midventricular area after myocardial infarction. In this study, we cannot provide detailed information about the cellular identity of these population, but a recent study showed, that after myocardial infarction 50% of S100A4 positive cells are hematopoietic cells and many endothelial cells are also S100A4 positive [10]. This could explain why some S100A4 positive cells co-localize with VEGF expression and some not. Clearly, future studies are needed to fully address this point and to identify the cellular identity of the cells.

Consistent with the in vivo data, cardiac myocyte death in response to oxidative stress was increased either when incubated in conditioned media from S100A4 KO fibroblasts or after siRNA-mediated knockdown of S100A4 in NRCMs. These data further suggest that paracrine factors (i.e. VEGF) from S100A4 positive cells (fibroblast, hematopoietic cells) or up-taken S100A4 itself regulate cellular survival in cardiac myocytes in response to stress. Multiple studies have shown that paracrine S100A4 can function via more than one cell surface receptor, possibly explaining its many and diverse effects. However, the nature of a cardiac S100A4 receptor is still unknown and remains a challenging direction for future studies. The healing process after ischemic injury involves complex and tight control of several signaling pathways. This response is necessary for healing and scar formation. Perturbations of this balance can lead to fatal complications including cardiac rupture in patients with myocardial infarction. Results presented in this study suggest that expression of S100A4 is necessary for this process, as genetic deletion of S100A4 increased cardiac damage. Molecularly, this could be mediated by an impaired angiogenesis response, which is important for proper healing [20,22]. In a previous study, loss of S100A4 led to decreased remodeling in response to pressure-overload, but in the present study, loss of S100A4 was not beneficial. Duration, intensity, and cell type-specific expression of S100A4 are potentially important for the effects of S100A4, and require further studies.

S100A4 is cardioprotective via increased AKT signaling.

S100A4 reduced ischemic injury in myocytes in part via increased AKT signaling (Fig. 4). Overall, our findings concur with previous reports of Akt-dependent cell survival and apoptosis [23]. The importance of S100A4 in tissue protection is also supported by recent reports that S100A4 protects neurons from cell death [16]. Furthermore, findings presented herein demonstrate that clinically relevant AAV-gene therapy with S100A4 is protective in response to infarction injury (Fig. 5). Importantly, S100A4 overexpression reduced infarction injury and improved cardiac function (Fig. 6). Recent advancements in the development of AAV vectors have enabled the first clinical trial with AAV based cardiac specific gene transfer [24,25]. Thus, cardio-protection by S100A4 could represent a future therapeutic option for treatment of myocardial injury.

Due to the focus of our study on early events after myocardial damage, several limitations are noteworthy. Detailed investigation of S100A4 potential impact on chronic myocardial remodeling and

survival is clearly needed, but was beyond the aim of the current study. Modulation of immune system activation by extracellular S100A4 will also be the subject of a future study, as S100A4 is highly expressed in hematopoietic cells. In addition, the effect on released pro-inflammatory and pro-fibrotic chemokines and cytokines awaits clarification. Overall, our study is the first linking S100A4 to cardio-protection in response to myocardial infarction.

5. Conclusions

Loss of viable myocardium after myocardial infarction is the leading cause of cardiac dysfunction resulting in chronic heart failure. Consequence of global deletion of S100A4 mice resulted in decreased cardiac function after myocardial infarction compared to control mice, whereas cardiac myocyte-specific overexpression of S100A4 protects the myocardium after infarction and improves cardiac function. Correctly-timed S100A4 therapy could be a potent combinatorial approach to blunt cellular losses and ameliorate progression of degenerative changes accompanying ischemic damage.

Contributions

S.D., M.A.S. and M.V. convinced and designed the study. M.K., N.G., H.T., L.O., D.T., conducted the experiments and performed analyses. C.C.G. devised experiments and commented on the manuscript. S.D., and M.V. wrote and finalized the manuscript.

Disclosures

None.

Acknowledgments

We would like to thank all members of the M.V. laboratory for helpful discussion and comments. This study was supported by Deutsche Forschungsgemeinschaft DFG to M.V. (1659/1-1) and to M.H.K. (3900/1-1), the National Institute of Health to M.A.S. (R21HL102714, R01HL067245, R37HL091102, P01HL085577, RC1HL100891, R21HL102613, R21HL104544, and R01HL105759) and to C.C.G. (RO1 HL75573, RO1 HL104535, RO3 EB011698), American Heart Association (11POST7610164), and the Rees-Stealy Research Foundation to S.D., P.Q. and the San Diego Chapter of the Achievement Rewards for College Scientists (ARCS) Foundation, the American Heart Association (Predoctoral Fellowship 10PRE3410005) and the Inamori Foundation to S.D.

Appendix A. Supplementary data

Supplementary data to this article can be found online at http://dx.doi.org/10.1016/j.yjmcc.2016.10.001.

References

[1] J.O. Mudd, D.A. Kass, Tackling heart failure in the twenty-first century, Nature 451 (2008) 919–928, http://dx.doi.org/10.1038/nature06798.
[2] M. Schneider, S. Kostin, C.C. Strøm, M. Aplin, S. Lyngbaek, J. Theilade, et al., S100A4 is upregulated in injured myocardium and promotes growth and survival of cardiac myocytes, Cardiovasc. Res. 75 (2007) 40–50, http://dx.doi.org/10.1016/j.cardiores.2007.03.027.
[3] R. Donato, Intracellular and extracellular roles of S100 proteins, Microsc. Res. Tech. 60 (2003) 540–551, http://dx.doi.org/10.1002/jemt.10296.
[4] K. Boye, G.M. Mælandsmo, S100A4 and metastasis: a small actor playing many roles, American Journal of Pathology (2009) http://dx.doi.org/10.2353/ajpath.2010.090526.
[5] J.T. O'Connell, H. Sugimoto, V.G. Cooke, B.A. MacDonald, A.I. Mehta, V.S. LeBleu, et al., VEGF-A and Tenascin-C produced by S100A4+ stromal cells are important for metastatic colonization, Proc. Natl. Acad. Sci. 108 (2011) 16002–16007, http://dx.doi.org/10.1073/pnas.1109493108.
[6] H. Wang, L. Duan, Z. Zou, H. Li, S. Yuan, X. Chen, et al., Activation of the PI3K/Akt/mTOR/p70S6K pathway is involved in S100A4-induced viability and migration in colorectal cancer cells, Int J Med Sci. 11 (2014) 841–849, http://dx.doi.org/10.7150/ijms.8128.
[7] G.S. Delassus, H. Cho, J. Park, G.L. Eliceiri, New pathway links from cancer-progression determinants to gene expression of matrix metalloproteinases in breast cancer cells, J. Cell. Physiol. 217 (2008) 739–744, http://dx.doi.org/10.1002/jcp.21548.
[8] M. Stary, M. Schneider, S.P. Sheikh, G. Weitzer, Parietal endoderm secreted S100A4 promotes early cardiomyogenesis in embryoid bodies, Biochem. Biophys. Res. Commun. 343 (2006) 555–563, http://dx.doi.org/10.1016/j.bbrc.2006.02.161.
[9] K. Song, Y.-J. Nam, X. Luo, X. Qi, W. Tan, G.N. Huang, et al., Heart repair by reprogramming non-myocytes with cardiac transcription factors, Nature 485 (2012) 599–604, http://dx.doi.org/10.1038/nature11139.
[10] P. Kong, P. Christia, A. Saxena, Y. Su, N.G. Frangogiannis, Lack of specificity of fibroblast-specific protein 1 in cardiac remodeling and fibrosis, AJP: Heart and Circulatory Physiology 305 (2013) H1363–H1372, http://dx.doi.org/10.1152/ajpheart.00395.2013.
[11] Y. Tamaki, Y. Iwanaga, S. Niizuma, T. Kawashima, T. Kato, Y. Inuzuka, et al., Metastasis-associated protein, S100A4 mediates cardiac fibrosis potentially through the modulation of p53 in cardiac fibroblasts, J. Mol. Cell. Cardiol. 57 (2013) 72–81, http://dx.doi.org/10.1016/j.yjmcc.2013.01.007.
[12] C.E.L. Naaman, B. Grum-Schwensen, A. Mansouri, M. Grigorian, E. Santoni-Rugiu, T. Hansen, et al., Cancer predisposition in mice deficient for the metastasis-associated Mts1(S100A4) gene, Oncogene 23 (2004) 3670–3680, http://dx.doi.org/10.1038/sj.onc.1207420.
[13] S. Doroudgar, M. Völkers, D.J. Thuerauf, M. Khan, S. Mohsin, J.L. Respress, et al., Hrd1 and ER-associated protein degradation, ERAD, are critical elements of the adaptive ER stress response in cardiac myocytes, Circ. Res. 117 (2015) 536–546, http://dx.doi.org/10.1161/CIRCRESAHA.115.306993.
[14] D. Matsubara, T. Niki, S. Ishikawa, A. Goto, E. Ohara, T. Yokomizo, et al., Differential expression of S100A2 and S100A4 in lung adenocarcinomas: clinicopathological significance, relationship to p53 and identification of their target genes, Cancer Sci. 96 (2005) 844–857, http://dx.doi.org/10.1111/j.1349-7006.2005.00121.x.
[15] K. Zhang, M. Zhang, H. Zhao, B. Yan, D. Zhang, J. Liang, S100A4 regulates motility and invasiveness of human esophageal squamous cell carcinoma through modulating the AKT/Slug signal pathway, Dis. Esophagus 25 (2012) 731–739, http://dx.doi.org/10.1111/j.1442-2050.2012.01323.x.
[16] O. Dmytriyeva, S. Pankratova, S. Owczarek, K. Sonn, V. Soroka, C.M. Ridley, et al., The metastasis-promoting S100A4 protein confers neuroprotection in brain injury, Nat. Commun. 3 (2012) 1197, http://dx.doi.org/10.1038/ncomms2202.
[17] J. Klingelhöfer, H.D. Møller, E.U. Sumer, C.H. Berg, M. Poulsen, D. Kiryushko, et al., Epidermal growth factor receptor ligands as new extracellular targets for the metastasis-promoting S100A4 protein, FEBS J. 276 (2009) 5936–5948, http://dx.doi.org/10.1111/j.1742-4658.2009.07274.x.
[18] M. Schneider, J.L. Hansen, S.P. Sheikh, S100A4: a common mediator of epithelial-mesenchymal transition, fibrosis and regeneration in diseases? J. Mol. Med. 86 (2008) 507–522, http://dx.doi.org/10.1007/s00109-007-0301-3.
[19] R.R. Yammani, D. Long, R.F. Loeser, Interleukin-7 stimulates secretion of S100A4 by activating the JAK/STAT signaling pathway in human articular chondrocytes, Arthritis Rheum. 60 (2009) 792–800, http://dx.doi.org/10.1002/art.24295.
[20] D. Yan, X. Wang, D. Li, W. Liu, M. Li, Z. Qu, et al., Macrophages overexpressing VEGF target to infarcted myocardium and improve neovascularization and cardiac function, Int. J. Cardiol. 164 (2013) 334–338, http://dx.doi.org/10.1016/j.ijcard.2011.07.026.
[21] H.-H. Lin, Y.-H. Chen, P.-F. Chang, Y.-T. Lee, S.-F. Yet, L.-Y. Chau, Heme oxygenase-1 promotes neovascularization in ischemic heart by coinduction of VEGF and SDF-1, J. Mol. Cell. Cardiol. 45 (2008) 44–55, http://dx.doi.org/10.1016/j.yjmcc.2008.04.011.
[22] Y.-D. Lin, C.-Y. Luo, Y.-N. Hu, M.-L. Yeh, Y.-C. Hsueh, M.-Y. Chang, et al., Instructive nanofiber scaffolds with VEGF create a microenvironment for arteriogenesis and cardiac repair, Sci Transl Med. 4 (2012), 146ra109 http://dx.doi.org/10.1126/scitranslmed.3003841.
[23] M. Völkers, M.H. Konstandin, S. Doroudgar, H. Toko, P. Quijada, S. Din, et al., mTORC2 protects the heart from ischemic damage, Circulation (2013) http://dx.doi.org/10.1161/CIRCULATIONAHA.113.003638.
[24] C.A. Pacak, B.J. Byrne, AAV vectors for cardiac Gene transfer: experimental tools and clinical opportunities, Mol. Ther. 19 (2009) 1582–1590, http://dx.doi.org/10.1038/mt.2011.124.
[25] B.E. Jaski, M.L. Jessup, D.M. Mancini, T.P. Cappola, D.F. Pauly, B. Greenberg, et al., Calcium upregulation by percutaneous administration of gene therapy in cardiac disease (CUPID Trial), a first-in-human phase 1/2 clinical trial, J. Card. Fail. 15 (2009) 171–181, http://dx.doi.org/10.1016/j.cardfail.2009.01.013.

Glossary

AAV: adeno associated Virus
ACM: adult cardiac myocytes
EF: ejection fraction
FB: fibroblasts
FS: fractional shortening
KO: knockout
LVEDP: left ventricular end diastolic pressure
LV: left ventricle
MI: myocardial infarction
NRCM: neonatal rat cardiac myocytes
TUNEL: terminal deoxynucleotidyl transferase dUTP nick end labeling
VEGF: vascular endothelial growth factor